Talanta 206 (2020) 120179

Contents lists available at ScienceDirect

Talanta

journal homepage: www.elsevier.com/locate/talanta

Synthesis of magnetic amino-functionalized microporous organic network composites for magnetic solid phase extraction of endocrine disrupting chemicals from water, beverage bottle and juice samples

Zong-Da Du[a], Yuan-Yuan Cui[a], Cheng-Xiong Yang[a,*], Xiu-Ping Yan[b]

[a] College of Chemistry, Research Center for Analytical Sciences, Tianjin Key Laboratory of Molecular Recognition and Biosensing, Nankai University, Tianjin, 300071, China

[b] State Key Laboratory of Food Science and Technology, International Joint Laboratory on Food Safety, Institute of Analytical Food Safety, School of Food Science and Technology, Jiangnan University, Wuxi, 214122, China

ARTICLE INFO

Keywords:
Microporous organic network
Composite
Magnetic solid phase extraction
Endocrine disrupting chemicals

ABSTRACT

In this work, the magnetic amino-functionalized microporous organic network composites (Fe_3O_4@MON-NH_2) were rational designed and facile synthesized for magnetic solid phase extraction (MSPE) of endocrine disrupting chemicals (EDCs), followed by their analysis with high-performance liquid chromatography. The incorporation of amino groups (hydrogen bonding sites) into hydrophobic MON-NH_2 networks led to their good enrichment for four typical EDCs bisphenol A (BPA), 4-alpha-cumylphenol (4-*α*-CP), 4-tert-octylphenol (4-*t*-OP) and 4-nonylphenol (4-NP) relying on the pre-designed hydrogen bonding, π-π and hydrophobic interactions. The combination of MON-NH_2 shell and magnetic Fe_3O_4 core provided a fast extraction of BPA, 4-α-CP, 4-*t*-OP and 4-NP from matrix solution. Under the optimal conditions, the developed method offered good linearity ($R^2 > 0.990$) in the range of 0.05–1000 μg L^{-1}, low limits of detection (S/N = 3) of 0.015–0.030 μg L^{-1} and large enrichment factors of 172–197 for the studied EDCs. The maximum adsorption capacities of BPA, 4-α-CP, 4-*t*-OP and 4-NP were 124.1, 105.6, 116.6 and 117.9 mg g^{-1}, respectively. The Fe_3O_4@MON-NH_2 gave larger selectivity for other polar phenols than non-polar polycyclic aromatic hydrocarbons, revealing the dominant role of hydrogen bonding interaction during the extraction and the potential of Fe_3O_4@MON-NH_2 for other polar phenols. The developed method was successfully applied for the analysis of EDCs in water, orange juice and beverage bottle samples with the recoveries of 80.3–109.5%. These results revealed the potential of functional MONs as efficient adsorbents in sample pretreatment.

1. Introduction

Endocrine disrupting chemicals (EDCs) are artificial chemicals that can cause endocrine system disorder and reproductive health damage [1,2]. Due to their widely distributing in the environment and the potential health problems [3–5], EDCs have received great concerns recently. Bisphenol A (BPA), 4-alpha-cumylphenol (4-α-CP), 4-*tert*-octylphenol (4-*t*-OP) and 4-nonylphenol (4-NP) are the four most typical phenolic EDCs. BPA is one of the highest-yield chemicals in the world (about 5–6 billion pounds per year) [6]. 4-CP is commonly used as stabilizers in the production of oils, polymers and rubber [7]. 4-*t*-OP and 4-NP are widely used as nonionic surfactants in many industries [8]. These phenolic EDCs are also the main industrial raw materials for the production of polycarbonates (PCs), which are widely used in the manufacture of baby bottles, plastic tableware, medical equipment and milk tanks [9]. Even if there are low levels of EDCs in the environment, they will pose a great threat to human health through direct contact and gradual accumulation [6–8]. Therefore, many provisions have been made for the concentration of these EDCs in terms of drinking water and food. The concentration of BPA should not be exceed 10.0 μg L^{-1} in drinking water according to the Chinese standard and the concentration of 4-NP is limited to 6.6 μg L^{-1} in drinking water according to US EPA [9]. So, it is essential to accurately monitor the EDCs' levels in environment.

However, direct detection of EDCs in environmental samples is usually difficult due to the complex matrix interference and low concentration of EDCs [10]. Proper sample pretreatment strategies are required before the quantitative analysis of EDCs. Many sample pretreatment techniques such as solid phase extraction (SPE) [1,2,9,11–13], liquid phase extraction (LPE) [8] and liquid-liquid

* Corresponding author.
E-mail address: cxyang@nankai.edu.cn (C.-X. Yang).

https://doi.org/10.1016/j.talanta.2019.120179
Received 11 April 2019; Received in revised form 7 July 2019; Accepted 24 July 2019
Available online 24 July 2019
0039-9140/

extraction (LLE) [14] have been explored for the pretreatment of EDCs. SPE is the most widely used pretreatment technique for EDCs because of the simple operation and less organic solvents consumption [15–23]. The adsorbent is the core of SPE. Development of highly efficient and selective adsorbents is quite important and challenging in SPE. Until now, many kinds of adsorbents including MCM-48 [18], MIPs-E1 [19], fBC [20], SBA-15-C_{18}-CO [21], bamboo charcoal [22] and metal-organic framework MIL-101 [23] have been explored for SPE of EDCs.

Cumbersome centrifugation and separation steps are still required during the SPE procedure. Magnetic nanoparticle-based magnetic separation has drawn great attention due to its rapid separation from the matrix, good reusability and low cost [6,24]. Magnetic SPE (MSPE) [1,2,9,25–33], a sub-class of SPE, has been quickly developed for sample pretreatment in diverse domains. To date, magnetic adsorbents such as Fe_3O_4@COF (TpBD) [1], Fe_3O_4/rGO [2], Fe@MgAl-LDH [9], Fe_3O_4@SiO_2-MIP [25], molecularly imprinted polymers [27–30] and Fe_3O_4-mPMF [33] have been studied for the MSPE of EDCs.

Benzene rings, –OH groups and hydrophobic alkyl chains are involved in BPA, 4-α-CP, 4-*t*-OP, 4-NP and many other EDCs' structures. Hydrogen bonding, π-π and hydrophobic interactions are the main adsorption mechanisms for EDCs [34,35]. Microporous organic networks (MONs) are a novel class of microporous materials with the merits of large surface area, good thermal and solvent stabilities, and easy engineering on other matrixes. Until now, MONs and MONs' composites such as MIL-101@MON [11], Co@C [36], UiO-66@MON [37], and MON [38–40] have been used as the efficient adsorbents for the adsorption and extraction of harmful pollutants in diverse matrixes. The hydrophobic MONs may be potential in SPE of EDCs with aromatic benzene rings and hydrophobic alkyl chains. In addition, integration of hydrogen bonding sites within aromatic and hydrophobic MONs' networks may largely promote their extraction performance for EDCs.

To this end, here we report the facile synthesis of magnetic amino-functionalized MON composites (Fe_3O_4@MON-NH_2) for efficient MSPE followed by high-performance liquid chromatography (HPLC) determination of four typical EDCs in water, beverage bottle and juice samples. The MON-NH_2 shell provides the hydrogen bonding, π-π and hydrophobic interaction sites for the selected four EDCs. The magnetic Fe_3O_4 core ensures the rapid separation from aqueous solution under external magnetic field. The experimental parameters such as adsorbents dosage, pH, extraction time, ionic strength, desorption solvent and volume that affecting the MSPE of EDCs were optimized in detail. The developed method gave good linearity, low limits of detection and large enrichment factors for the studied EDCs. Determination of EDCs in water, beverage bottle and orange juice samples were also realized. These results revealed the potential of functional MONs as efficient adsorbents in sample pretreatment.

2. Experimental

2.1. Reagents and materials

All reagents were at least of analytical grade. Ethylene glycol (EG), $FeCl_3{\cdot}6H_2O$, Poly (4-styrenesulfonic acid-co-maleic acid) sodium salt (PSSMA 3:1, *M*w 20000), 2,5-dibromobenzenamine, 1,4-diiodobenzene, copper (I) iodide, 3-nitrophenol (3-NP), *p*-chlorophenol (*p*-CP), 2,6-dichlorophenol (2,6-DCP), 2,3-dichlorophenol (2,3-DCP), naphthalene (Nap), acenaphthene (Ace), fluoranthene (FluA), pyrene (Pyr), and triethylamine were purchased from Aladdin Chemistry Co., Ltd. (Shanghai, China). Tetrakis (4-ethynylphenyl) methane was bought from Chengdu Tongchuangyuan Pharmaceutical Technology Co. (Chengdu, China). Toluene was obtained from Chemical Reagent Sixth Factory (Tianjin, China). Bisphenol A (BPA), 4-alpha-Cumylphenol (4-α-CP), 4-*tert*-octylphenol (4-*t*-OP), 4-nonylphenol (4-NP) and bis(triphenylphosphine)palladium (II) chloride were purchased from TCI Chemical Industry Development Co. (Shanghai, China). Ultrapure water was supplied by Wahaha Foods Co. Ltd. (Tianjin, China). Methanol (HPLC grade), ethanol, isopropanol, acetonitrile and dichloromethane were obtained from Concord Technology (Tianjin, China).

2.2. Instrumentation

The chromatographic system consisted of a Waters 510 pump and a 486 tunable UV detector. The EDCs were separated on a Baseline C18 column (4.6 mm i.d. × 25 cm long, Tianjin, China) at a flow rate of 1.0 mL min^{-1} using methanol: water (v/v, 9/1) as the mobile phase. The UV detector was set at 227 nm. The X-ray diffraction spectrometry (XRD) patterns were recorded on a D/max-2500 diffractometer (Rigaku, Japan) from 3° to 80°. The magnetic hysteresis loops were studied on a LDJ 9600-1 vibrating sample magnetometer (VSM) (LDJ Electronics Inc Troy, MI, USA) at room temperature by cycling the field from −10 to 10 kOe. Thermogravimetric analysis (TGA) was performed on a PTC-10A thermal gravimetric analyzer (Rigaku, Japan) from room temperature to 700 °C. The transmission electron microscopy (TEM) image was recorded on Tecnai G2 F20 (Philips, Holland) at 200 kV. The N_2 adsorption-desorption experiments were recorded on a NOVA 2000e surface area and pore size analyzer (Quantachrome, USA) at 77 K.

2.3. Synthesis of Fe_3O_4@MON-NH_2

The magnetic Fe_3O_4 nanospheres were prepared according to the previous reported solvothermal method [35]. Briefly, 10 mL EG solution of 0.81 g $FeCl_3{\cdot}6H_2O$ and 1.8 g of sodium acetate were mixed with 10 mL EG solution of 0.7 g PSSMA. The mixture was then transferred into a Teflon stainless steel autoclave and stayed at 200 °C for 10 h. After cooling to room temperature, the dark product was separated by a magnet, washed with water and ethanol, and then dried under vacuum overnight.

The facile synthesis of Fe_3O_4@MON-NH_2 was depicted in Fig. 1a. Fe_3O_4 nanospheres (0.10 g), $Pd(PPh_3)_2Cl_2$ (1.7 mg, 2.4 μmol) and CuI (0.50 mg, 2.6 μmol) were dispersed with triethylamine (7.5 mL) and toluene (7.5 mL) in a 100 mL three-necked flask. The mixture was sonicated for 30 min and mechanically stirred at a stirring rate of 500 rpm under 90 °C for 30 min. Tetrakis (4-ethynylphenyl) methane (25.0 mg, 0.06 mmol) and 2,5-dibromobenzenamine (30.1 mg, 0.12 mmol) were then added. The mixture was mechanically stirred at 90 °C for 5 h. After cooling to room temperature, the obtained Fe_3O_4@MON-NH_2 was separated by a magnet, washed three times with dichloromethane and methanol, and dried under vacuum overnight. Fe_3O_4@MON was prepared under the same conditions by changing 2,5-dibromobenzenamine to 1,4-diiodobenzene.

2.4. Sample preparation

The stock solutions of BPA, 4-α-CP, 4-*t*-OP and 4-NP (1 mg mL^{-1} for each) were prepared with methanol and stored at 4 °C in the dark [41]. The working solution was prepared from the stock solution by stepwise dilution with ultrapure water and small amount of methanol. The content of methanol was gradually reduced during the dilution process. The volume portion of methanol in any working solution was kept less than 1% [41].

The river and lake water samples were collected from local XinKai Lake (Tianjin, China) and Weijin River (Tianjin, China). The water samples were filtered with 0.22 μm Millipore cellulose membrane immediately after sampling. The orange juice samples (Meinianda, PepsiCo) were purchased from local supermarket (Tianjin, China). The orange juice samples were filtered with 0.22 μm Millipore cellulose membrane before use [42]. The beverage bottle water extract was prepared as follows. The used beverage bottle (Wahaha) was filled with boiling water and then stayed overnight to get beverage bottle water extract sample. The water sample was filtered with 0.22 μm Millipore cellulose membrane before use.

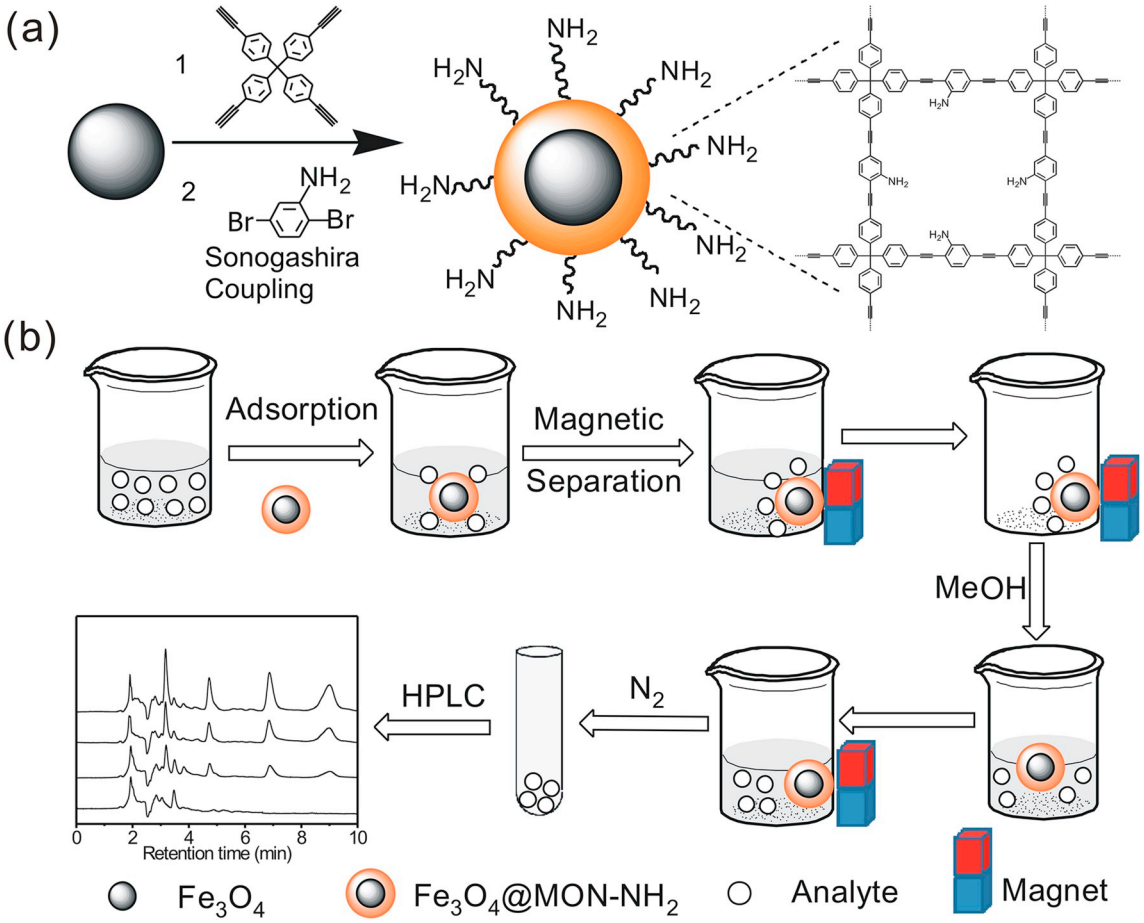

Fig. 1. Illustration of (a) the synthesis of Fe_3O_4@MON-NH_2 and (b) their application in MSPE of EDCs.

2.5. MSPE procedures

The MSPE procedures were depicted in Fig. 1b. Typically, 4 mg of Fe_3O_4@MON-NH_2 was mixed with 20 mL of sample solution. The mixture was shaken (200 rpm) for 40 min in a water bath at 25 °C to extract the target EDCs. Then, the Fe_3O_4@MON-NH_2 was collected with a magnet and the supernatant was completely discarded. The adsorbed EDCs were desorbed from the Fe_3O_4@MON-NH_2 with 0.4 mL of methanol (0.2 mL × 2) under ultrasonication for 20 s. The eluent was concentrated to 0.1 mL under N_2 flow and then sampled for HPLC analysis.

3. Results and discussion

3.1. Characterization of Fe_3O_4@MON-NH_2

The synthesized Fe_3O_4@MON-NH_2 was characterized with TEM, XRD, N_2 adsorption-desorption experiments, TGA and magnetization curves (Fig. 2). The TEM images of Fe_3O_4 and Fe_3O_4@MON-NH_2 were shown in Fig. 2a–b. The results revealed the core-shell structure of Fe_3O_4@MON-NH_2. The uniform MON-NH_2 shell with a thickness of about 40 nm was well coated on Fe_3O_4 core (Fig. 2b). The XRD pattern of Fe_3O_4@MON-NH_2 exhibited the characteristic face-centered cubic peaks of Fe_3O_4 in the range of 20–70° (Fig. 2c), suggesting the successful synthesis of Fe_3O_4@MON-NH_2 [35]. The Brunauer-Emmett-Teller (BET) surface area of Fe_3O_4@MON-NH_2 was 370.6 $m^2 g^{-1}$ (Fig. 2d). The appearance of the characteristic peaks at 589 cm^{-1} for Fe–O, and 1494 cm^{-1} for C–N in the FT-IR spectra of Fe_3O_4@MON-NH_2 revealed the successful formation of MON-NH_2 shell on Fe_3O_4 (Fig. S1) [27,43]. The TGA curve showed the synthesized Fe_3O_4@MON-NH_2 was stable up to 300 °C (Fig. 2e). The M_s values of Fe_3O_4 and Fe_3O_4@MON-NH_2 were 70 and 48 emu g^{-1}, respectively (Fig. 2f). There were no apparent hysteresis, remanence and coercivity in the hysteresis loops of Fe_3O_4 and Fe_3O_4@MON-NH_2. The large M_s value of Fe_3O_4@MON-NH_2 made it convenient for magnetic separation.

3.2. Effect of Fe_3O_4@MON-NH_2 dosage

Effect of Fe_3O_4@MON-NH_2 dosage on the extraction efficiency of BPA, 4-α-CP, 4-*t*-OP and 4-NP was studied (Fig. 3a). The peak areas increased with the increasing amount of Fe_3O_4@MON-NH_2 from 1 to 4 mg, and then leveled off or even decreased slightly as the amount of Fe_3O_4@MON-NH_2 was larger than 4 mg. The decrease of the extraction efficiency may be due to the fact that some of the EDCs on Fe_3O_4@MON-NH_2 had not been fully desorbed [8]. Therefore, 4 mg of Fe_3O_4@MON-NH_2 was selected in subsequent experiments.

3.3. Effect of pH

The pH of the solution was an important factor affecting the MSPE efficiency. The pH would influence the dissociation of phenolic EDCs in aqueous solution and then further affect the extraction efficiency of phenolic EDCs on adsorbents [8]. Therefore, effect of pH on MSPE of BPA, 4-α-CP, 4-*t*-OP and 4-NP on Fe_3O_4@MON-NH_2 was investigated in the pH range of 4–10 (Fig. 3b). The results showed that the peak areas of BPA, 4-α-CP, 4-*t*-OP and 4-NP changed little in the pH range of 4–8, suggesting the stable extraction efficiency of Fe_3O_4@MON-NH_2 for EDCs in neutral and weakly acidic environments. However, the peak areas of BPA, 4-α-CP, 4-*t*-OP and 4-NP decreased as the pH values increased from 9 to 10, showing the alkaline condition was not favorable

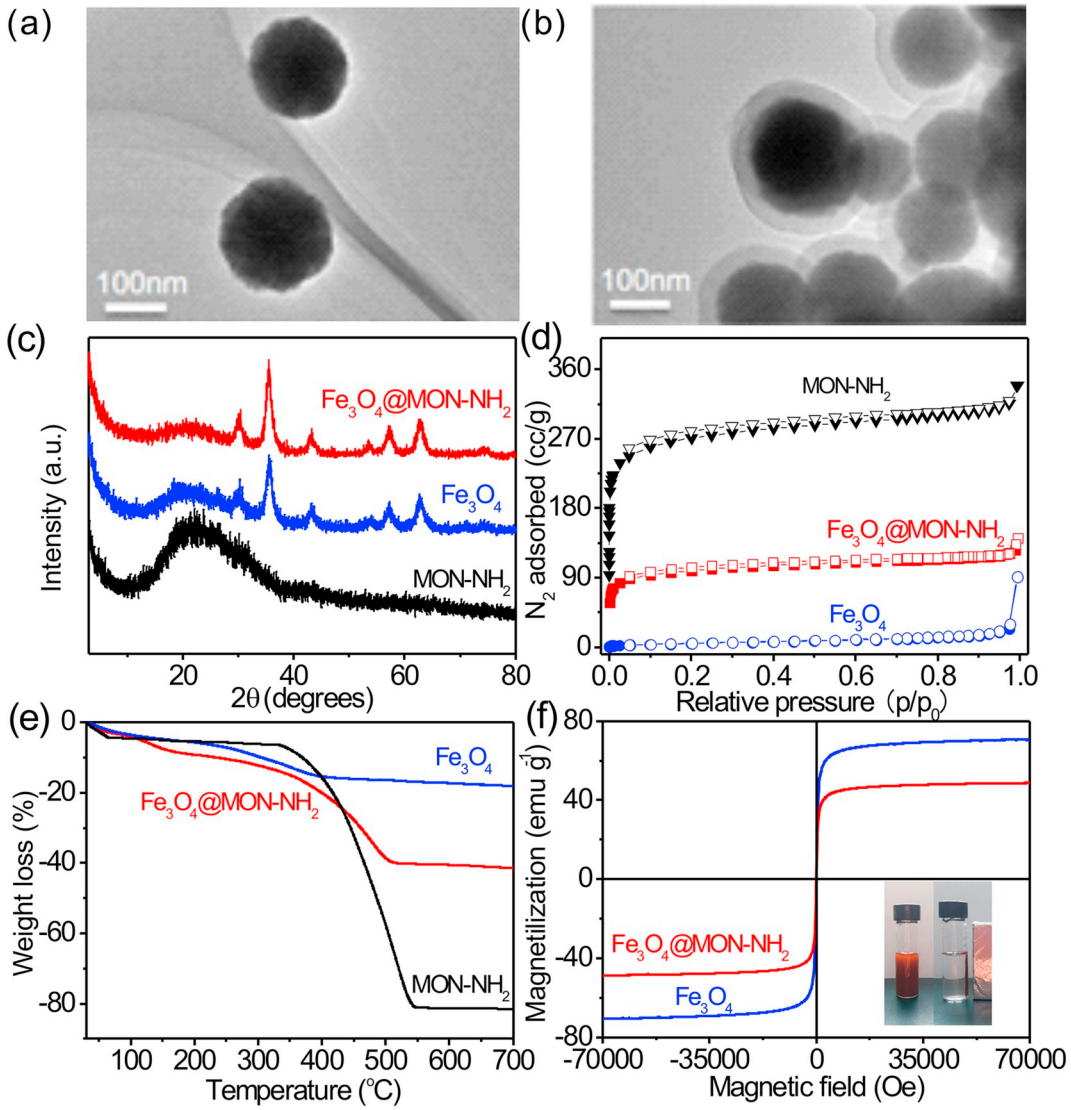

Fig. 2. TEM images of (a) Fe_3O_4 and (b) Fe_3O_4@MON-NH_2; (c) XRD patterns, (d) N_2 adsorption-desorption isotherms and (e) TGA curves of MON-NH_2, Fe_3O_4 and Fe_3O_4@MON-NH_2; (f) magnetization curves of Fe_3O_4 and Fe_3O_4@MON-NH_2.

for MSPE of these EDCs on Fe_3O_4@MON-NH_2. The pKa values of these phenolic EDCs were about 10 [8]. When pH = 9, the phenolic hydroxyl groups on EDCs started to dissociate, leading to the decrease of the hydrogen bonding interaction between EDCs and Fe_3O_4@MON-NH_2. Thus, decrease of the extraction efficiency of EDCs on Fe_3O_4@MON-NH_2. Considering that the pH values of the water samples investigated in this study were neutral or acidic, the pH of sample solution in this work was not adjusted.

3.4. Effect of extraction time

Effect of extraction time on the extraction efficiency of BPA, 4-α-CP, 4-*t*-OP and 4-NP on Fe_3O_4@MON-NH_2 was then evaluated (Fig. 3c). The peak areas of BPA, 4-α-CP, 4-*t*-OP and 4-NP increased as the extraction time increased from 10 to 40 min. Further increase of the extraction time to 50 min led to no significant increase of peak areas for the studied EDCs, suggesting that the extraction equilibrium was achieved within 40 min. Therefore, 40 min was chosen as the extraction time.

3.5. Effect of ionic strength

Effect of ionic strength on MSPE of BPA, 4-α-CP, 4-*t*-OP and 4-NP on Fe_3O_4@MON-NH_2 was further studied in the NaCl concentration range of 0–100 mM (Fig. 3d). The peak areas of BPA, 4-α-CP, 4-*t*-OP and 4-NP changed little as the concentration of NaCl increased from 0 to 100 mM, showing the good anti-interference property of Fe_3O_4@MON-NH_2. In general, increase of the NaCl concentration may lead to the decrease of the EDCs' solubility in aqueous phase, which was favorable for their transformation or extraction on Fe_3O_4@MON-NH_2 [41]. However, the added NaCl could also increase the matrix effect and solution viscosity and then decrease the diffusion rate, which was negative for their transformation or extraction on Fe_3O_4@MON-NH_2. Therefore, no NaCl was added in subsequent experiments.

3.6. Effects of desorption solvent and volume

Methanol, acetonitrile and isopropanol were chosen as the desorption solvents to desorb the adsorbed BPA, 4-α-CP, 4-*t*-OP and 4-NP from Fe_3O_4@MON-NH_2 (Fig. 3e). The methanol gave the best desorption efficiency to the studied EDCs. Effect of methanol volume on the desorption of BPA, 4-α-CP, 4-*t*-OP and 4-NP from Fe_3O_4@MON-NH_2 was further studied (Fig. 3f). The results showed that 0.4 mL of methanol (0.2 mL × 2) was sufficient to desorb the adsorbed EDCs from Fe_3O_4@MON-NH_2.

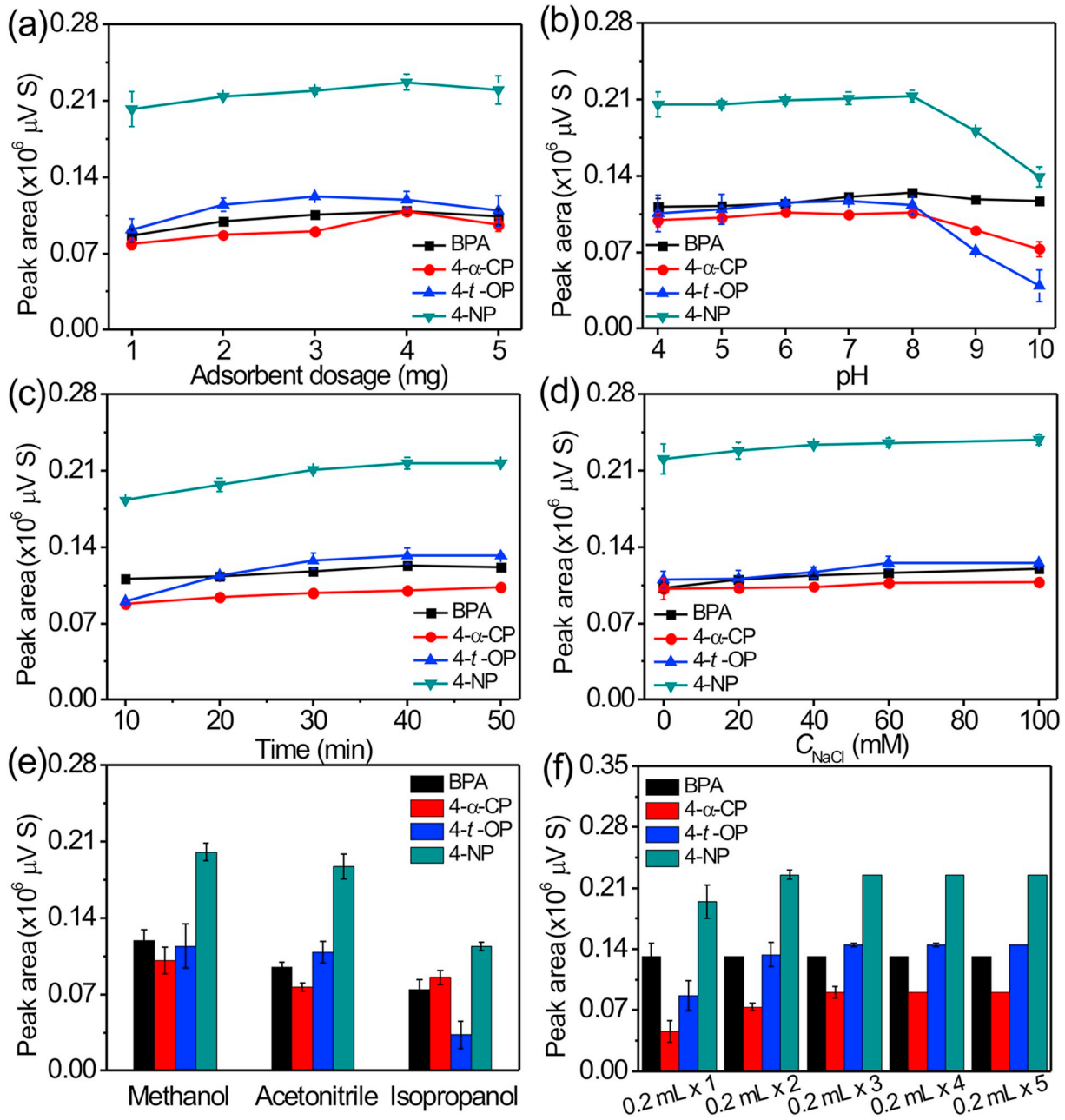

Fig. 3. Effects of (a) Fe_3O_4@MON-NH_2 dosage, (b) pH, (c) extraction time, (d) ionic strength, (e) desorption solvent and (f) methanol volume on the MSPE of EDCs on Fe_3O_4@MON-NH_2. The concentrations of spiked BPA, 4-α-CP, 4-*t*-OP and 4-NP are 50, 50, 100 and 250 μg L^{-1}, respectively. Error bars show the standard deviations for three replicate extractions.

3.7. Method validation

The figures of merits for the MSPE using Fe_3O_4@MON-NH_2 as the sorbent for HPLC determination of EDCs were summarized in Table 1. The linear range of proposed method for the determination of BPA, 4-α-CP, 4-*t*-OP and 4-NP were 0.05–200, 0.05–200, 0.10–400 and 0.10–1000 μg L^{-1}, respectively. The precisions (RSDs, %) for intra-day (n = 5) and inter-day (n = 4) were 1.2–6.1% and 3.2–8.7%, respectively. A series of standard EDCs solutions (0.01–1000 μg L^{-1}) were prepared to determine the limits of detection (LOD) and limits of quantification (LOQ) of the proposed method [44]. The LODs of EDCs were determined by reducing the EDCs' concentration until levels were reached based on signal-to-noise ratio (S/N) of 3. The LOQs were determined at a signal-to-noise ratio of 10. The lowest concentration on the calibration curve should be accepted as LOQ [44]. The LODs and LOQs for the studied EDCs were 0.015–0.030 μg L^{-1} and 0.050–0.100 μg L^{-1}, respectively. The enhancement factors (EFs) were defined as the ratio of the sensitivity (peak area) of an analyte after extraction to that before extraction [41]. The Fe_3O_4@MON-NH_2 gave large EFs of 197, 172, 196 and 192 for BPA, 4-α-CP, 4-*t*-OP and 4-NP,

Table 1
Parameters of the proposed MSPE method for the determination of EDCs.

EDCs	Linear range (μg L^{-1})	Calibration equation[a]	R^2	Precision (RSDs)[b] (%)		LODs (μg L^{-1})	LOQs (μg L^{-1})
				Intra-day n = 5	Inter-day n = 4		
BPA	0.050–200	y = 2256.8x + 369.9	0.999	1.2	3.2	0.015	0.050
4-α-CP	0.050–200	y = 1857.2x + 420.6	0.997	3.2	7.4	0.015	0.050
4-*t*-OP	0.100–400	y = 1663.7x + 412.0	0.991	4.4	5.2	0.030	0.100
4-NP	0.100–1000	y = 903.5x + 267.9	0.992	6.1	8.7	0.030	0.100

[a] y: peak area (μV S), x: concentration of EDCs (μg L^{-1}).
[b] The concentration of spiked BPA, 4-α-CP, 4-*t*-OP and 4-NP are 10, 10, 20 and 50 μg L^{-1},respectively.

Table 2
EFs values of the proposed MSPE method for EDCs using Fe_3O_4, Fe_3O_4@MON and Fe_3O_4@MON-NH_2 as the adsorbents.

EDCs	EFs (means ± *s*, *n* = 3)[a]		
	Fe_3O_4	Fe_3O_4@MON	Fe_3O_4@MON-NH_2
BPA	23 ± 1	138 ± 2	197 ± 3
4-α-CP	23 ± 1	125 ± 6	172 ± 3
4-*t*-OP	22 ± 1	132 ± 7	196 ± 6
4-NP	12 ± 2	135 ± 1	192 ± 7

[a] The concentration of spiked BPA, 4-α-CP, 4-*t*-OP and 4-NP are 10, 10, 20 and 50 μg L^{-1},respectively.

respectively (Table 2). The maximum adsorption capacity of BPA, 4-α-CP, 4-*t*-OP and 4-NP were 124.1, 105.6, 116.6 and 117.9 mg g^{-1}, respectively (Fig. S2, Table S1). Furthermore, the peak areas of BPA, 4-α-CP, 4-*t*-OP and 4-NP decreased only 9.6%, 7.2%, 13.4% and 10.1% after four adsorption-desorption cycles (Fig. 4a), indicating the good reusability of Fe_3O_4@MON-NH_2 for EDCs. Compared with other reported methods [1,2,9,22,25,45,46], the developed MSPE-HPLC method gave wider linear range, lower LODs and less adsorbent consumption (Table 3). The less adsorbent dosage, good reusability and extraction efficiency made Fe_3O_4@MON-NH_2 low-cost and potential in sample pretreatment.

3.8. Adsorption mechanisms

To evaluate the adsorption mechanisms of Fe_3O_4@MON-NH_2 for EDCs, the MSPE of these EDCs on Fe_3O_4 and Fe_3O_4@MON were compared (Fig. 4b). The bare Fe_3O_4 gave poor extraction for EDCs with the EFs of 12–23 (Table 2), suggesting the MON-NH_2 shell on Fe_3O_4@MON-NH_2 played key roles during the extraction. The Fe_3O_4@MON without amino groups provided higher extraction efficiency and larger EFs (125–138) than the bare Fe_3O_4 for EDCs, showing the π-π and hydrophobic interactions between EDCs and Fe_3O_4@MON were taken place during the extraction. In addition, the Fe_3O_4@MON-NH_2 showed higher extraction efficiency and larger EFs (172–197) than those on Fe_3O_4@MON for the studied EDCs, further demonstrating the significant roles of hydrogen bonding interaction between the hydroxyl groups on EDCs and amino groups on Fe_3O_4@MON-NH_2.

The pKa values of BPA, 4-α-CP, 4-*t*-OP, and 4-NP were 9.5, 10.1, 10.3 and 10.7, respectively [8]. The BPA, 4-α-CP, 4-*t*-OP, and 4-NP were exited as neutral or undissociated form in the pH range of 4–8 (pH < pKa), which were favorable to form hydrogen bonding (N···H···O) interaction between –NH_2 groups on Fe_3O_4@MON-NH_2 and –OH groups on EDCs [47]. However, the BPA, 4-α-CP, 4-*t*-OP, and 4-NP were started to dissociate when the pH larger than 9. The dissociation of the hydroxyl group would weaken the hydrogen bonding interaction between Fe_3O_4@MON-NH_2 and phenolic EDCs, thereby decreasing the extraction efficiency. These results revealed that the hydrogen bonding, π-π and hydrophobic interactions all played important roles for the high efficiency extraction for the studied EDCs.

To further evaluate the extraction mechanisms and the selectivity of Fe_3O_4@MON-NH_2, the MSPE of non-polar polycyclic aromatic hydrocarbons (PAHs) and polar phenols on Fe_3O_4@MON-NH_2 was studied (Table S2). The Fe_3O_4@MON-NH_2 gave lower EFs to PAHs than phenols, further revealing the dominant role of hydrogen bonding interaction during the MSPE. In addition, the EFs of the studied PAHs were in the range of 100–115, showing the π-π and hydrophobic interactions between PAHs and Fe_3O_4@MON-NH_2 were also taken place during the extraction. These results also showed the potential of Fe_3O_4@MON-NH_2 for MSPE of the polar phenols.

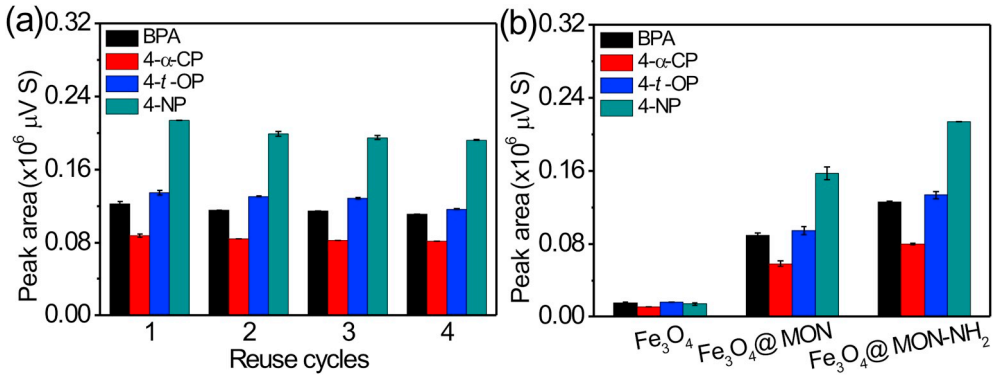

Fig. 4. (a) Reusability of Fe_3O_4@MON-NH_2 for EDCs; (b) MSPE of EDCs on Fe_3O_4, Fe_3O_4@MON and Fe_3O_4@MON-NH_2. The concentrations of spiked BPA, 4-α-CP, 4-*t*-OP and 4-NP are 50, 50, 100 and 250 μg L^{-1}, respectively.

Table 3
Comparison of the developed method with other methods for the determination of EDCs.

Adsorbents	Extraction mode	Analytes	Dosage (mg)	Analytical technique	Linearity (μg L^{-1})	Recovery (%)	RSD (%)	LODs (μg L^{-1})	Ref
Bamboo charcoal	SPE	BPA, 4-*t*-OP, 4-NP		HPLC-UV	2–100	79.5–104.3	3.0–5.6	0.17–0.37	[22]
C_{18}	SPE	BPA, 4-*t*-OP, 4-NP	500	HPLC-MS/MS	1–100	95.0–107.0	4.1–15.2	0.15–0.32	[45]
Fe_3O_4@TpBD	MSPE	BPA, 4-NP	10	HPLC-FLD	10–1000	90.4–101.6	1.7–6.3	2.30–4.00	[1]
Fe_3O_4/rGO	MSPE	4-*t*-OP	100	GC-MS	2.5–100	96.3–112.6	2.8–6.5	1.23	[2]
Fe@MgAl-LDH	MSPE	BPA, 4-*t*-OP, 4-NP	50	HPLC-UV	0.5–200	96.0–96.3	1.2–2.3	0.24–0.34	[9]
Fe_3O_4@SiO_2-MIP	MSPE	BPA	40	HPLC-UV		97.2–99.2	2.9–3.8	3.70	[25]
Gn-MNPs	MSPE	4-NP	80	HPLC-VWD	0.1–500	93.0–101.1	1.2–2.5	0.017	[46]
Fe_3O_4@MON-NH_2	MSPE	BPA, 4-α-CP, 4-*t*-OP, 4-NP	4	HPLC-UV	0.05–1000	81.0–107.4	1.2–6.1	0.015–0.030	This work

3.9. Real sample analysis

To evaluate the practical applicability of the established MSPE method, the determination of these EDCs in lake water, river water, beverage bottle water extract and juice samples were performed (Fig. 5, Table 4). Although there were complex matrices in these real samples (Fig. 5), these matrices did not affect the detection of EDCs as their retention times were different to the studied EDCs. The BPA with the concentration of 0.3 μg L^{-1} was detected in beverage bottle water extract (Fig. 5d, Table 4). The recoveries of EDCs in three spiked levels are in the range of 80.3%–109.5%. The concentrations of EDCs in the real water sample after spiking (x values) were calculated via the calibration equations in Table 1 as their peak areas (y values) could be obtained by HPLC analysis. These results indicated the availability of the developed MSPE-HPLC method for the determination of EDCs in real samples.

4. Conclusion

In summary, we have reported the design and synthesis of magnetic Fe_3O_4@MON-NH_2 composites for MSPE of BPA, 4-α-CP, 4-*t*-OP and 4-NP in water and juice samples. Depending on the pre-designed hydrogen bonding, π-π and hydrophobic interaction sites in MON-NH_2 shell and magnetic Fe_3O_4 core, the Fe_3O_4@MON-NH_2 gave large adsorption capacity and enrichment efficiency for the studied phenolic EDCs with good linearity and precisions, less adsorbent consumption and low LODs. The proposed method also showed lower LODs and less adsorbent consumption than many other reported methods. These results reveal the feasibility and potential of functionalized MONs in sample pretreatment. Although off-line MSPE could reduce the cumbersome centrifuging and separation steps during the SPE procedure, the inherent disadvantages of off-line SPE may still hinder its further application. On-line SPE should be an effective way to overcome the

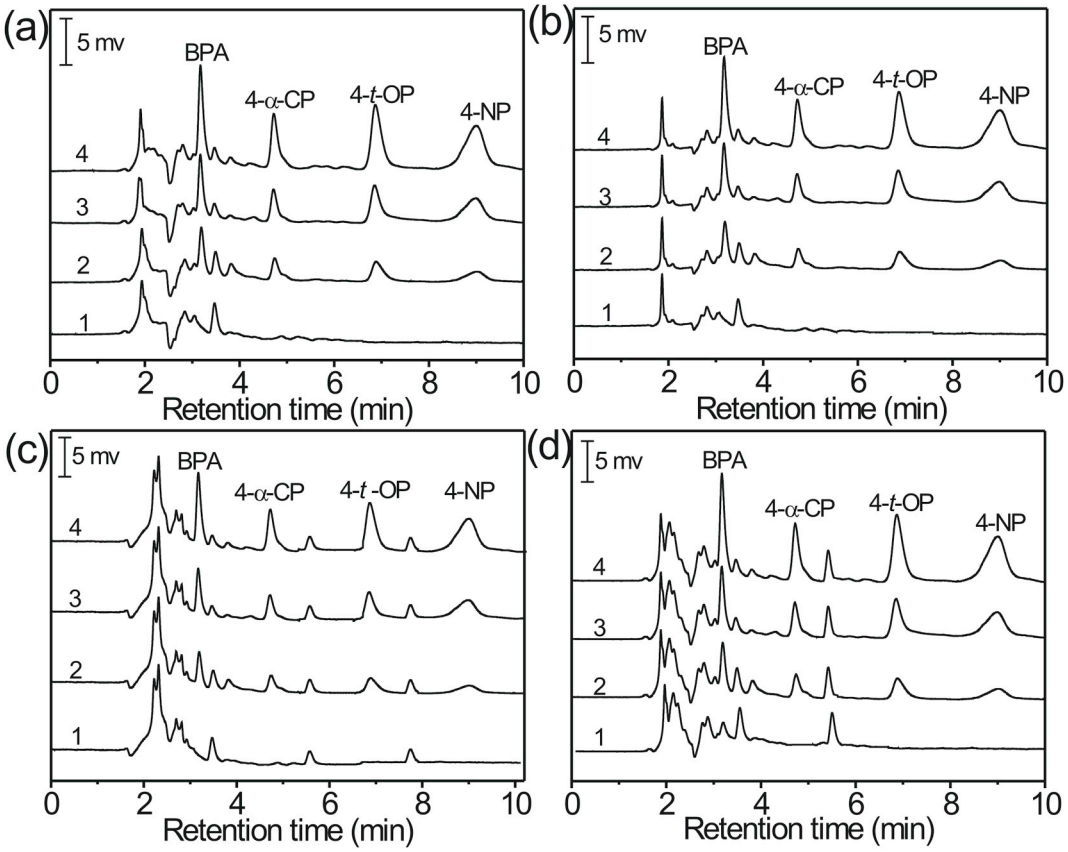

Fig. 5. HPLC chromatograms of Fe_3O_4@MON-NH_2 for MSPE-HPLC determination of EDCs in (a) river water, (b) lake water, (c) orange juice and (d) beverage bottle water extract samples. The concentration of spiked EDCs is depicted in Table 4.

Table 4
Analytical results for the determination of EDCs in river water, lake water, juice and beverage bottle samples ($n=3$).

EDCs	Spiked ($\mu g\ L^{-1}$)	Recovery ± SD (%, $n=3$)			
		River water	Lake water	Juice	Beverage bottle
BPA	0[b]	nd[a]	nd	nd	0.30 ± 0.04
	10[b]	83.2 ± 1.6	86.3 ± 1.9	88.1 ± 1.0	81.7 ± 2.5
	25[b]	83.0 ± 1.3	81.0 ± 0.3	81.7 ± 0.3	85.9 ± 3.1
	50[b]	84.9 ± 0.7	81.2 ± 1.9	82.5 ± 0.9	88.0 ± 2.2
4-α-CP	0	nd	nd	nd	nd
	10	98.1 ± 4.7	94.0 ± 1.6	93.0 ± 5.6	85.3 ± 2.0
	25	101.5 ± 3.5	81.7 ± 2.5	89.4 ± 0.2	87.4 ± 0.8
	50	96.8 ± 1.5	82.2 ± 0.5	80.3 ± 0.3	90.9 ± 2.2
4-*t*-OP	0	nd	nd	nd	nd
	20	107.4 ± 2.7	95.7 ± 0.9	82.8 ± 1.1	95.4 ± 3.2
	50	97.8 ± 2.6	83.5 ± 0.5	88.4 ± 1.2	81.9 ± 1.8
	100	103.5 ± 1.5	90.2 ± 1.6	100.4 ± 1.1	100.1 ± 3.7
4-NP	0	nd	nd	nd	nd
	50	84.0 ± 2.8	98.1 ± 1.1	85.0 ± 1.6	85.5 ± 1.7
	125	109.5 ± 0.5	93.2 ± 1.1	91.1 ± 4.8	87.4 ± 0.5
	250	99.8 ± 1.2	96.8 ± 1.3	84.7 ± 0.4	83.7 ± 4.0

[a] Not detected.
[b] The concentration of spiked EDCs was corresponded to the 1, 2, 3, and 4 in Fig. 5.

above-mentioned disadvantages. Rational design and synthesis of functional MONs for on-line SPE should be a prospect area in the sample pretreatment.

Notes

The authors declare no competing financial interest.

Acknowledgements

This work was supported by the National Key Research and Development Program of China (No. 2018YFC1602401), the National Natural Science Foundation of China (Nos. 21777074 and 21775056), the National Basic Research Program of China (No. 2015CB932001), Tianjin Natural Science Foundation (No. 18JCQNJC05700) and the Fundamental Research Funds for Central Universities.

Appendix A. Supplementary data

Supplementary data to this article can be found online at https://doi.org/10.1016/j.talanta.2019.120179.

References

[1] N. Li, D. Wu, J. Liu, N. Hu, X. Shi, C. Dai, Z. Sun, Y. Suo, G. Li, Y. Wu, Magnetic covalent organic frameworks based on magnetic solid phase extraction for determination of six steroidal and phenolic endocrine disrupting chemicals in food samples, Microchem. J. 143 (2018) 350–358.
[2] E.Ö. Er, A. Çağlak, G.Ö. Engin, S. Bakirdere, Ultrasound-assisted dispersive solid phase extraction based on Fe_3O_4/reduced graphene oxide nanocomposites for the determination of 4-*tert* octylphenol and atrazine by gas chromatography-mass spectrometry, Microchem. J. 146 (2019) 423–428.
[3] J. Annamalai, V. Namasivayam, Endocrine disrupting chemicals in the atmosphere: their effects on humans and wildlife, Environ. Int. 76 (2015) 78–97.
[4] A. Ghassabian, L. Trasande, Disruption in thyroid signaling pathway: a mechanism for the effect of endocrine-disrupting chemicals on child neurodevelopment, Front. Endocrinol. 9 (2018) 204.
[5] A. Nadal, E. Fuentes, C. Ripoll, S. Villar-Pazos, M. Castellano-Munoz, S. Soriano, J. Martinez-Pinna, I. Quesada, P. Alonso-Magdalena, Extranuclear-initiated estrogenic actions of endocrine disrupting chemicals: is there toxicology beyond paracelsus? J. Steroid Biochem. 176 (2018) 16–22.
[6] O. Filippou, E.A. Deliyanni, V.F. Samanidou, Fabrication and evaluation of magnetic activated carbon as adsorbent for ultrasonic assisted magnetic solid phase dispersive extraction of bisphenol A from milk prior to high performance liquid chromatographic analysis with ultraviolet detection, J. Chromatogr. A 1479 (2017) 20–31.
[7] T. Janicki, M. Krupinski, J. Dlugonski, Degradation and toxicity reduction of the endocrine disruptors nonylphenol, 4-*tert*-octylphenol and 4-cumylphenol by the non-ligninolytic fungus Umbelopsis isabellina, Bioresour. Technol. 200 (2016) 223–229.
[8] Q. Zhou, Y. Gao, G. Xie, Determination of bisphenol A, 4-n-nonylphenol, and 4-*tert*-octylphenol by temperature-controlled ionic liquid dispersive liquid-phase microextraction combined with high performance liquid chromatography-fluorescence detector, Talanta 85 (3) (2011) 1598–1602.
[9] Q. Zhou, M. Lei, J. Li, K. Zhao, Y. Liu, Sensitive determination of bisphenol A, 4-nonylphenol and 4-octylphenol by magnetic solid phase extraction with Fe@MgAl-LDH magnetic nanoparticles from environmental water samples, Separ. Purif. Technol. 182 (2017) 78–86.
[10] A. Azzouz, A.J. Rascon, E. Ballesteros, Simultaneous determination of parabens, alkylphenols, phenylphenols, bisphenol A and triclosan in human urine, blood and breast milk by continuous solid-phase extraction and gas chromatography-mass spectrometry, J. Pharmaceut. Biomed. 119 (2016) 16–26.
[11] Y. Jia, H. Su, Z. Wang, Y.E. Wong, X. Chen, M. Wang, T.D. Chan, Metal-organic framework@microporous organic network as adsorbent for solid-phase microextraction, Anal. Chem. 88 (19) (2016) 9364–9367.
[12] A.G. Asimakopoulos, N.S. Thomaidis, Bisphenol A, 4-t-octylphenol, and 4-nonylphenol determination in serum by hybrid solid phase extraction-precipitation technology technique tailored to liquid chromatography-tandem mass spectrometry, J. Chromatogr. B 986–987 (2015) 85–93.
[13] W.K. Meng, L. Liu, X. Wang, R.S. Zhao, M.L. Wang, J.M. Lin, Polyphenylene core-conjugated microporous polymer coating for highly sensitive solid-phase microextraction of polar phenol compounds in water samples, Anal. Chim. Acta 1015 (2018) 27–34.
[14] O.G. Sas, I. Dominguez, B. Gonzalez, A. Dominguez, Liquid-liquid extraction of phenolic compounds from water using ionic liquids: literature review and new experimental data using [C_2mim] FSI, J. Environ. Manag. 228 (2018) 475–482.
[15] E.A. Dil, M. Ghaedi, A. Asfaram, F. Mehrabi, A.A. Bazrafshan, Optimization of process parameters for determination of trace hazardous dyes from industrial wastewaters based on nanostructures materials under ultrasound energy, Ultrason. Sonochem. 40 (2018) 238–248.
[16] E.A. Dil, M. Ghaedi, A. Asfaram, A. Goudarzi, Synthesis and characterization of ZnO-nanorods loaded onto activated carbon and its application for efficient solid phase extraction and determination of BG from water samples by micro-volume spectrophotometry, New J. Chem. 39 (12) (2015) 9407–9414.
[17] F. Mehrabi, A. Vafaei, M. Ghaedi, A.M. Ghaedi, E.A. Dil, A. Asfaram, Ultrasound assisted extraction of Maxilon Red GRL dye from water samples using cobalt ferrite nanoparticles loaded on activated carbon as sorbent: optimization and modeling, Ultrason. Sonochem. 38 (2017) 672–680.
[18] S. Zhang, F. Lu, X. Ma, M. Yue, Y. Li, J. Liu, J. You, Quaternary ammonium-functionalized MCM-48 mesoporous silica as a sorbent for the dispersive solid-phase extraction of endocrine disrupting compounds in water, J. Chromatogr. A 1557 (2018) 1–8.
[19] X. Wang, P. Huang, X. Ma, X. Du, X. Lu, Enhanced in-out-tube solid-phase microextraction by molecularly imprinted polymers-coated capillary followed by HPLC for endocrine disrupting chemicals analysis, Talanta 194 (2019) 7–13.
[20] M.B. Ahmed, J.L. Zhou, H.H. Ngo, M.A.H. Johir, K. Sornalingam, Sorptive removal of phenolic endocrine disruptors by functionalized biochar: competitive interaction mechanism, removal efficacy and application in wastewater, Chem. Eng. J. 335 (2018) 801–811.
[21] J. Ganan, S. Morante-Zarcero, D. Perez-Quintanilla, M.L. Marina, I. Sierra, One-pot synthesized functionalized mesoporous silica as a reversed-phase sorbent for solid-phase extraction of endocrine disrupting compounds in milks, J. Chromatogr. A 1428 (2016) 228–235.
[22] R.S. Zhao, X. Wang, J.P. Yuan, L.L. Zhang, Solid-phase extraction of bisphenol A, nonylphenol and 4-octylphenol from environmental water samples using microporous bamboo charcoal, and their determination by HPLC, Microchim. Acta 165 (3–4) (2009) 443–447.
[23] S.C. Tan, H.K. Lee, A metal-organic framework of type MIL-101(Cr) for emulsification-assisted micro-solid-phase extraction prior to UHPLC-MS/MS analysis of polar estrogens, Microchim. Acta 186 (3) (2019) 165.
[24] M. Cao, P. Wang, Y. Ao, C. Wang, J. Hou, J. Qian, Photocatalytic degradation of tetrabromobisphenol A by a magnetically separable graphene-TiO_2 composite photocatalyst: mechanism and intermediates analysis, Chem. Eng. J. 264 (2015) 113–124.
[25] Y. Yuan, Y. Liu, W. Teng, J. Tan, Y. Liang, Y. Tang, Preparation of core-shell magnetic molecular imprinted polymer with binary monomer for the fast and selective extraction of bisphenol A from milk, J. Chromatogr. A 1462 (2016) 2–7.
[26] L. Zhou, Y. Hu, G. Li, Conjugated microporous polymers with built-in magnetic nanoparticles for excellent enrichment of trace hydroxylated polycyclic aromatic hydrocarbons in human urine, Anal. Chem. 88 (13) (2016) 6930–6938.
[27] H. Gholami, M. Arabi, M. Ghaedi, A. Ostovan, A.R. Bagheri, Column packing elimination in matrix solid phase dispersion by using water compatible magnetic molecularly imprinted polymer for recognition of melamine from milk samples, J. Chromatogr. A 1594 (2019) 13–22.
[28] A.R. Bagheri, M. Arabi, M. Ghaedi, A. Ostovan, X. Wang, J. Li, L. Chen, Dummy molecularly imprinted polymers based on a green synthesis strategy for magnetic solid-phase extraction of acrylamide in food samples, Talanta 195 (2019) 390–400.
[29] M. Arabi, M. Ghaedi, A. Ostovan, Development of a lower toxic approach based on green synthesis of water-compatible molecularly imprinted nanoparticles for the extraction of hydrochlorothiazide from human urine, ACS Sustain. Chem. Eng. 5 (5) (2017) 3775–3785.
[30] M. Arabi, A. Ostovan, M. Ghaedi, M.K. Purkait, Novel strategy for synthesis of magnetic dummy molecularly imprinted nanoparticles based on functionalized

silica as an efficient sorbent for the determination of acrylamide in potato chips: optimization by experimental design methodology, Talanta 154 (2016) 526–532.
[31] E.A. Dil, M. Ghaedi, A. Asfaram, Application of hydrophobic deep eutectic solvent as the carrier for ferrofluid: a novel strategy for pre-concentration and determination of mefenamic acid in human urine samples by high performance liquid chromatography under experimental design optimization, Talanta 202 (2019) 526–530.
[32] E.A. Dil, A. Asfaram, F. Sadeghfar, Magnetic dispersive micro-solid phase extraction with the CuO/ZnO@Fe_3O_4-CNTs nanocomposite sorbent for the rapid pre-concentration of chlorogenic acid in the medical extract of plants, food, and water samples, Analyst 144 (8) (2019) 2684–2695.
[33] Y. Song, R. Ma, C. Jiao, L. Hao, C. Wang, Q. Wu, Z. Wang, Magnetic mesoporous polymelamine-formaldehyde resin as an adsorbent for endocrine disrupting chemicals, Microchim. Acta 185 (1) (2017) 19.
[34] X.H. Zhu, C.X. Yang, X.P. Yan, Metal-organic framework-801 for efficient removal of fluoride from water, Microporous Mesoporous Mater. 259 (2018) 163–170.
[35] Y. Li, C.X. Yang, X.P. Yan, Controllable preparation of core-shell magnetic covalent-organic framework nanospheres for efficient adsorption and removal of bisphenols in aqueous solution, Chem. Commun. 53 (16) (2017) 2511–2514.
[36] S. Hong, J. Yoo, N. Park, S.M. Lee, J.G. Park, J.H. Park, S.U. Son, Hollow Co@C prepared from a Co-ZIF@microporous organic network: magnetic adsorbents for aromatic pollutants in water, Chem. Commun. 51 (100) (2015) 17724–17727.
[37] J. Chun, S. Kang, N. Park, E.J. Park, X. Jin, K.D. Kim, H.O. Seo, S.M. Lee, H.J. Kim, W.H. Kwon, Y.K. Park, J.M. Kim, Y.D. Kim, S.U. Son, Metal-organic framework@microporous organic network: hydrophobic adsorbents with a crystalline inner porosity, J. Am. Chem. Soc. 136 (19) (2014) 6786–6789.
[38] N. Kang, J.H. Park, M. Jin, N. Park, S.M. Lee, H.J. Kim, J.M. Kim, S.U. Son, Microporous organic network hollow spheres: useful templates for nanoparticulate Co_3O_4 hollow oxidation catalysts, J. Am. Chem. Soc. 135 (51) (2013) 19115–19118.
[39] J. Li, H. Li, Y. Zhao, S. Wang, X. Chen, R.S. Zhao, A hollow microporous organic network as a fiber coating for solid-phase microextraction of short-chain chlorinated hydrocarbons, Microchim. Acta 185 (9) (2018) 416.
[40] J.Q. Ma, L. Liu, X. Wang, L.Z. Chen, J.M. Lin, R.S. Zhao, Development of dispersive solid-phase extraction with polyphenylene conjugated microporous polymers for sensitive determination of phenoxycarboxylic acids in environmental water samples, J. Hazard Mater. 371 (2019) 433–439.
[41] S.H. Huo, X.P. Yan, Facile magnetization of metal-organic framework MIL-101 for magnetic solid-phase extraction of polycyclic aromatic hydrocarbons in environmental water samples, Analyst 137 (15) (2012) 3445–3451.
[42] J. Wang, L. Hao, C. Wang, Q. Wu, Z. Wang, Nanoporous carbon as the solid-phase extraction adsorbent for the extraction of endocrine disrupting chemicals from juice samples, Food Anal. Method 10 (8) (2017) 2710–2717.
[43] G. Zhao, Y. Cheng, Y. Wu, X. Xu, X. Hao, New 2D carbon nitride organic materials synthesis with huge-application prospects in CN photocatalyst, Small 14 (15) (2018) 1704138.
[44] S. Chandran, R.S.P. Singh, Comparison of various international guidelines for analytical method validation, Pharmazie 62 (1) (2007) 4–14.
[45] F. Zhou, L. Zhang, A. Liu, Y. Shen, J. Yuan, X. Yu, X. Feng, Q. Xu, C. Cheng, Measurement of phenolic environmental estrogens in human urine samples by HPLC-MS/MS and primary discussion the possible linkage with uterine leiomyoma, J. Chromatogr. B 938 (2013) 80–85.
[46] Y. Wu, C. Chen, Q. Zhou, Q.X. Li, Y. Yuan, Y. Tong, H. Wang, X. Zhou, Y. Sun, X. Sheng, Polyamidoamine dendrimer decorated nanoparticles as an adsorbent for magnetic solid-phase extraction of tetrabromobisphenol A and 4-nonylphenol from environmental water samples, J. Colloid Interface Sci. 539 (2019) 361–369.
[47] L. Ji, L. Zhou, X. Bai, Y. Shao, G. Zhao, Y. Qu, C. Wang, Y. Li, Facile synthesis of multiwall carbon nanotubes/iron oxides for removal of tetrabromobisphenol A and Pb (ii), J. Mater. Chem. 22 (31) (2012) 15853.